International Journal of Computing and Digital Systems
ISSN (2210-142X)
Int. J. Com. Dig. Sys. #, No.# (Mon-20..)

High Impedance Fault Detection in Microgrid to Enhance Resiliency Against PMU Outage

Laxman Solankee[1], Dr. Avinash Rai[2] and Dr. Mukesh Kirar[3]

[1] *Department of Electrical Engineering, RGPV, Bhopal, M.P., India*
[2] *Department of Electronics and Communication, UIT, RGPV, Bhopal, M.P., India*
[3] *Department of Electrical, MANIT, Bhopal, M.P., India*

E-mail address: solankeelaxman@gmail.com, avinashrai@rgtu.net, kirarmk@gmail.com

Received ## Mon. 20##, Revised ## Mon. 20##, Accepted ## Mon. 20##, Published ## Mon. 20##

Abstract: High-impedance fault (HIF) detection is crucial for maintaining the reliability and resiliency of microgrid systems. This research presents an adaptive machine learning approach to enhance HIF detection and improve resiliency against the outage of optimally placed phasor measurement units (PMUs) in microgrids. PMUs are strategically positioned in limited numbers across the microgrid, considering their cost-effectiveness. When one of these PMUs encounters an outage, HIF detection becomes more complex due to the critical information loss from the affected area. The proposed approach utilizes a combined framework of correlation modelling, feature extraction using Hilbert-Huang Transformation (HHT), and Analysis of Variance (ANOVA). By leveraging machine learning algorithms, the approach selects the most relevant features derived from Hilbert spectral analysis (HSA) to perform tasks such as PMU outage detection, HIF detection, and classification during optimally placed PMU outage scenarios. The effectiveness of the approach in enhancing resiliency for high-impedance fault (HIF) detection during PMU outage scenarios is demonstrated through simulation studies conducted in MATLAB Simulink on microgrid systems.

Keywords: Microgrid, SCADA, PMU, Huang Hilbert Transformation, ANOVA, Protection Devices, Machine Learning.

1. INTRODUCTION

Phasor measurement units (PMUs) are intelligent electronic devices (IEDs) crucial for controlling and monitoring power networks in microgrid setups and provide synchronized phasors time tagged with the global positioning system (GPS) clocks[1]. While it would be optimal to install PMUs on every bus for comprehensive system monitoring, the high installation costs and limited communication infrastructure render this approach economically and practically unviable. To minimize expenses, PMUs are strategically placed on specific buses. These PMUs monitor and analyze data not only from their own bus but also from neighboring buses where PMUs are not deployed[2], [3]. However, in the event of a malfunction or damage to one of these PMUs, there is a risk of losing data from all interconnected buses, which can significantly impact the effectiveness of the centralized protection scheme.

In addition to the challenges posed by PMU deployment, high impedance faults (HIFs) further complicate the reliable operation of microgrids. Traditional fault detection methods often fail to detect HIFs due to their high impedance and low fault currents[4]. The situation becomes even more complex when HIFs occur on buses where a PMU is not deployed. Detecting such faults becomes challenging as the distance to the nearest PMU is greater, and the fault magnitude is already very low. Researchers have recently focused on applying machine learning algorithms to improve fault detection accuracy.

Several methods have been presented in the literature for solving the optimal PMU placement (OPP) problem such as genetic algorithm[5]–[10], particle swarm optimization (PSO)[11]–[13]imperialistic competition algorithm[14], chemical reaction optimization[15], TABU search [16] and Teaching–learning based optimization[17]. All of the approaches mentioned above have primarily focused on the optimal placement of PMUs, but no research work has, however, been validated by associating it with the detection and mitigation of high impedance faults (HIFs) during PMU outages.

Multiple research studies such as [4], [18]–[22], have examined the detection of high impedance faults (HIFs). However, these studies solely concentrate on HIF detection and have not addressed the crucial task of validating their effectiveness in detecting and mitigating HIFs during PMU outages. Therefore, there is currently no research that establishes a connection between HIF detection and effective fault mitigation in PMU outage scenarios.

The PMU data, on the other hand, may suffer from contamination by quasi-noise, which can lead to inaccurate results when used in power system applications by a phasor data concentrator (PDC). Additionally, there may be instances where data from PMUs to PDCs is missing[23]. In the NASPI design[24], measurements obtained from multiple PMUs are merged at PDCs, which then transmit the measurements to subsequent PDCs or the central control unit. Consequently, this disruption can result in either the control centre not receiving real-time data or raising suspicions about the validity of the measures. These factors undermine the observability and effectiveness of the centralized protection scheme [25]. To tackle these challenges, the proposed research aims to develop an innovative machine learning-based protection scheme. This scheme will provide resilience against misleading PMU data or system noise, as well as detect HIF in the system.

The proposed research work aims to enhance the effectiveness of microgrid protection using the Hilbert-Huang Transform (HHT) as a signal-processing technique for feature extraction and fault identification. To improve the efficiency of feature selection, a protection scheme combines the HHT with the Analysis of Variance (ANOVA) approach. This combined framework helps identify the most efficient features derived from the HHT, enabling accurate estimation of estate in Phasor Measurement Units (PMUs), specific fault detection, and section identification in the outage zone. To address the challenges of fault identification in complex scenarios, the proposed research incorporates machine learning-based algorithms. While a Decision Tree (DT) is a commonly used machine learning approach, it may not provide satisfactory performance for complex datasets. Hence, the research work explores the use of ensemble techniques to overcome this limitation. By employing an ensemble of decision trees, known as Bagging, the research work aims to improve classification and regression outcomes. Bagging combines individual Decision Tree results through a polling approach, where the majority of votes are considered for classification tasks, and mean values are used for regression tasks.

The following summarizes the important contributions/ highlights of the proposed research work.

- Development of a combined framework of HHT and ANOVA to select the most efficient features for various scenarios, such as estate estimation of PMUs, specific fault detection, and section identification in the outage zone.
- Development of a robust protection mechanism for a microgrid to provide resiliency against optimally placed PMU outage scenarios.
- Uncertain data from optimally placed PMUs are analyzed quantitatively using empirical decomposition (EMD) and Hilbert spectral analysis (HSA) functions, providing insights into data characteristics.
- The suggested protection technique is rigorously evaluated and compared to existing machine learning approaches, demonstrating its effectiveness across diverse situations.

The remainder of the paper is arranged as follows: Section 2 discusses the proposed protection methodology for the microgrid system. Section 3 focuses on the performance evaluation of the microgrid system. Lastly, Section 4 concludes the work.

2. PROPOSED PROTECTION METHODOLOGY FOR THE MICROGRID SYSTEM

Figure 1 illustrates a schematic representation of the microgrid 34.5 kV, 60 Hz system, simulated using MATLAB/Simulink. In islanded operation, both Zone-I and Zone-II are efficiently powered by two main sources of renewable energy: the 9.2 MW Photo Voltaic DG (PVDG2) at bus B7, along with a synchronous DG (SDGII) at bus B6, and PVDG1 located at bus B1, together with another synchronous DG (SDGI) at bus B3. These power generation systems are equipped with power conditioning units featuring a DC-DC converter, VSI, and phase-locked loop (PLL), ensuring a stable and reliable power supply to all the loads in their respective zones. Sections S1, S3, S5, and S7 span a length of 8 kilometres each, while Sections S2, S4, and S6 cover a distance of 12 kilometres each. The loads denoted as L1, L2, L3, L4, L5, L6, L7, and L8 represent the power consumption. PMUs 2 and 3 are optimally placed in zone I on buses B5 and B7, while PMU 1 is installed on bus B1. The GPS clock synchronizes all three PMUs. These PMUs gather comprehensive system information and transmit it to the PDC, which subsequently transfers the data to the central processing unit.

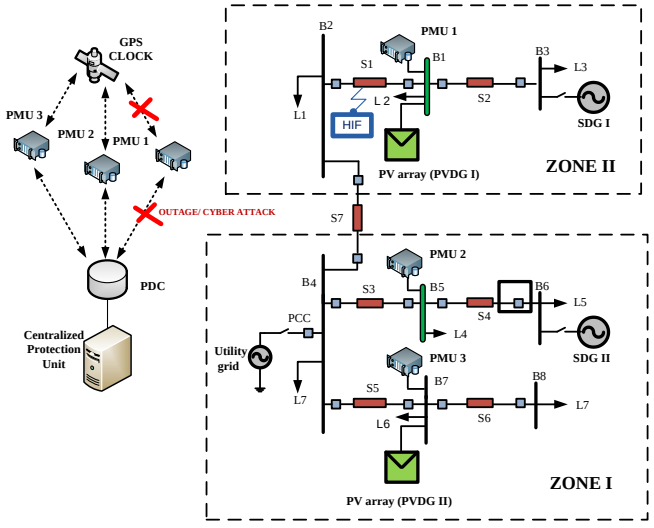

Fig 1. Microgrid Model

Figure 2 illustrates the PMU current data, including magnitude, angle, and frequency, measured at bus B1 (in red) and bus B7 (in green). A fault is introduced at 0.2 second in section 1 (S1). Notably, when measuring the current magnitude using the PMU1 at bus B1, it is significantly larger (shown in red); conversely, the magnitude is lower when measured by the PMU3 at bus B7 (shown in green). In case of a High Impedance Fault (HIF) at section S1 during PMU1 outage or in the presence of deceptive PMU data, the central protection unit is intelligently designed to utilize the joint framework model of PMU 2 and 3 to track PMU 1 estate estimation, fault detection, classification, and other related functionalities.

Some faults, like HIF and symmetrical faults (LLL and LLLG), are difficult to identify due to their similar current characteristics. Conventional relaying methods are ineffective in detecting these faults. The challenge becomes even more significant when trying to detect HIF faults from a considerable distance in another PMU zone, refer to Figure 3 for a visual depiction of the nonlinear characteristics associated with HIF.

Fig 3. Nonlinear characteristics associated with HIF.

Both Figure 4 and Figure 5 exhibit fault current patterns that are remarkably similar, presenting significant challenges for their identification through conventional relaying approaches. Figure 5 shows the phase A fault current variation during faults at the PVDG2 in section S5 and the distribution line fault (AG fault) in section S3 with R_f = 22 ohms. The measurements were captured using PMU3 at bus B7. Notably, both fault locations in the microgrid exhibit a similar fault current profile, as clearly depicted in the figure. Similarly, In Figure 4, the Microgrid shows similar fault current patterns for symmetrical faults like LLLG fault and LLL fault in section S3 measured at bus B7. Detecting these similar fault characteristics can be challenging, especially if the PMU in that zone is damaged. In such cases, it becomes more difficult to locate the fault using data from other PMUs.

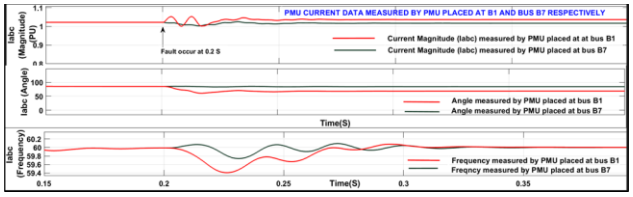

Fig. 2. PMU current data such as (a) magnitude (b) angle and (c) frequency measured at bus B1 is shown in red, while data measured at bus B7 is shown in green.

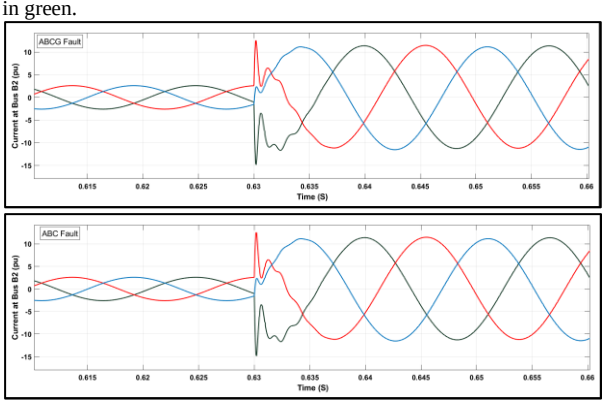

Fig. 4. Microgrid similar characteristic of LLL and LLLG fault in section S3 measured at bus B7 (a) ABCG fault (b) ABC fault

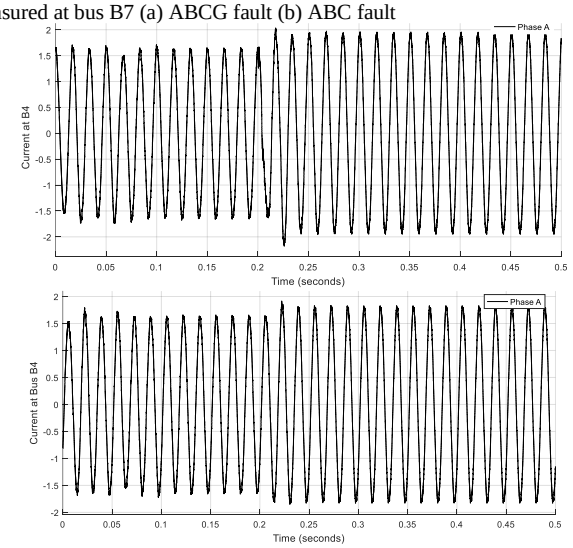

Fig. 5. Microgrid similar fault current profile of phase A measured at bus B7 during (a) PV array (PVDG2) fault in section S5 (b) Distribution line fault (AG fault) in section S3.

A. Protection Schemes Flowchart

Figure 6 illustrates a flowchart outlining a proposed protection scheme for microgrid systems. The raw time-domain three-phase instantaneous voltage and current data have been recorded by all the PMUs connected to the system.

The PMUs' acquired data signals will undergo a two-step decomposition using empirical mode decomposition (EMD) techniques and Hilbert-Huang Transformation (HHT). This process yields six parameters: intrinsic mode function 1 and 2 (IMF1 and IMF2), instantaneous frequency 1 and 2 (INSF1 and INSF2), and instantaneous energy 1 and 2 (INSE1 and INSE2), as depicted in Figures 7 and 8.

The decomposition process is iteratively applied to various circumstances, encompassing multiple fault scenarios, outages, PMU misleading data, and varying irradiance levels, with the results data being saved. Subsequently, essential characteristics of the signal, including mean, RMS, standard deviations (SD), shape factor, kurtosis, skewness, crest factor, impulse factor, clearance factor, peak value, SN ratio, THD, SINAD, and others, will be extracted. Among these, the ANOVA method will be employed, considering the specific circumstances, to identify the top 18 features for the state

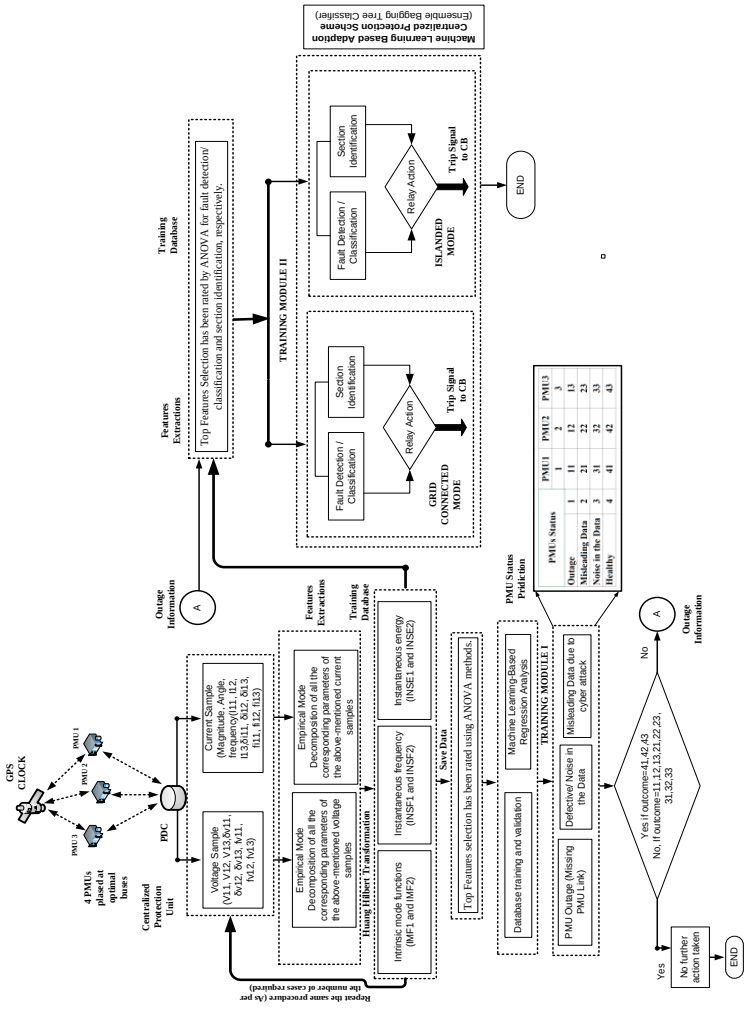

Fig. 6. Proposed protection schemes flowchart

estimation of PMUs. These features include SNR, THD, KURTOSIS for cuuent I_a, I_b, I_c and THD, Clearance Factor and SINAD for voltage V_a, V_b, and V_c. Following this, machine learning techniques will be utilized to determine the state of PMUs, such as outage, healthy status, misleading data, noise in the data, and more.

After receiving outage information, the top 18 features extraction process is repeated using ANOVA technique to identify the fault type and fault section within the outage PMU zone. The features considered include STD, SKEWNESS, and THD for phases I_a, I_b, I_c, and voltages V_a, V_b, and V_c. Subsequently, an ensemble bagging tree machine-learning algorithm is employed to accurately determine the exact fault type and fault section from adjacent PMUs.

B. Feature extraction by using the combined framework of EMD, HHT and ANOVA Technique

The signal decomposition technique known as HHT utilizes the EMD method to decompose the signal into intrinsic mode functions (IMFs). Subsequently, the Hilbert spectral analysis (HSA) is applied to these IMFs, resulting in the generation of instantaneous frequency (INSF) and instantaneous energy (INSE) data [26]. HHT is specifically designed to effectively handle nonstationary and nonlinear data. Moreover, Fourier transformations can be employed for preprocessing and decomposing data into mono-component elements. However, it is important to note that a limitation of this approach is that the Fourier transform only yields physically relevant components when the data exhibits linearity, stationarity, or absolute periodicity.

C. Empirical Mode Decomposition (EMD)

The EMD approach is employed to convert large-scale datasets into a collection of IMFs, which are then subjected to Hilbert spectral analysis. IMFs represent fundamental oscillatory modes, with each IMF exhibiting varying amplitude and frequency along the time axis, rather than a constant amplitude and frequency like a simple harmonic component. The process of obtaining an IMF is referred to as sifting [26]. The following outlines the sifting procedure:

a) Identify all of the local extrema in the signal data set. Fit an envelope through maxima, which is generally referred to as the upper envelope, and another envelope through minima, which is referred to as the lower envelope. The fitting is often performed using cubic spline functions.

$$Maxima: E_{max}(t) \quad (1)$$

$$Minima: E_{min}(t) \quad (2)$$

b) Find the average of the upper and lower envelopes' mean value denoted by S_{mean} *(t).*

$$S_{mean}(t) = E_{max}(t) + E_{min}(t) \quad (3)$$

c) Determine a residual value by subtracting the mean envelope from the original signal.

$$Res_{i+1}(t) = Res_i(t) - S_{mean}(t) \quad (4)$$

d) Verify the stop criterion: Huang et al. provided this criterion in 1998. It is identical to the Cauchy convergence test, and the sum of the differences, SD, is defined as

$$SD = \sum(t) = \frac{(Res_{i+1}(t) - Res_i(t))^2}{Res_i{}^2(t)} \quad (5)$$

The sifting operation is then terminated when the SD is less than a certain threshold value. The process is reiterated using the residual until the stopping requirement is satisfied. Following that, the first IMF decomposition (IMF1) is achieved. Repeat the process using the updated version of the original signal to generate the second decomposition of IMF (IMF2), and so on. The IMF fluctuates near zero, Only the non-zero mean component is the remaining residual, denoted by Res by (4). EMD provides IMFs as well as residuals. Higher mode numbers have higher scales and lower frequencies. The original signal is represented by the sum of all modes and the remaining residual is represented by (6). EMD for LLLG fault is depicted as shown in Figure 8, where n is the no. of modes.

$$Original\ Signal = \sum imf_n + Residual \quad (6)$$

D. Hilbert Spectral Analysis

After obtaining the IMFs components, the Hilbert transform can be used to calculate the instantaneous frequency. After applying the Hilbert transform to each IMF component, the original data may be described as the real portion, Real, as follows:

$$X(t) = Real \sum aj(t) e^{i \int wj(t) dt} \quad (7)$$

E. Hilbert spectral analysis for LLLG fault, Instantaneous frequency and instantaneous energy as illustrated in Figure 7 One-Way Analysis of Variance (ANOVA)

The one-way ANOVA is used to identify the best features from a large set of options such as kurtosis, signal to noise ratio (SNR), clearance factor, impulse factor, THD, standard deviation etc. It evaluates the mean value of all extracted features and analyzes if any of those means are significantly different from each other. It specifically examines the null hypothesis:

$$H_o = \mu 1 = \mu 2 = \mu 3 = \cdots = \mu$$

.

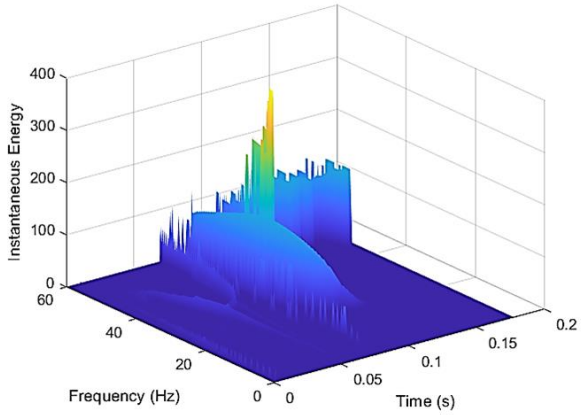

Fig. 7. Hilbert spectral analysis for LLLG fault

Where μ is the mean of the group and 1,2,3 is the number of features, the alternative hypothesis (HA), which asserts that the means of at least two features significantly differ from each other.

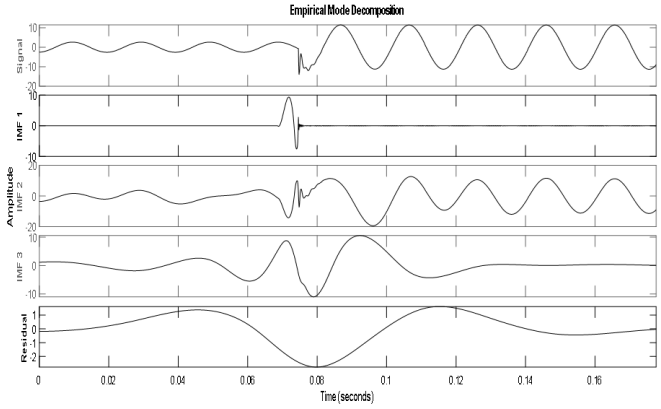

Fig. 8. Empirical Mode Decomposition for LLLG fault

3. PERFORMANCE EVALUATION FOR THE MICROGRID GRID SYSTEM

A. PMU Estate Estimation

Table I showcases the performance of the proposed PMU estate estimation training module I for the microgrid system. In the event of any misleading or noise in the PMU data, the central protection scheme will detect and isolate the respective faulty PMU. However, if there are only load fluctuations or the PMU readings are accurate, the central protection scheme remains unaffected and does not require modification.

TABLE I: RESPONSE OF PROPOSED TRAINING MODULE I IN THE OCCURRENCE OF A PMU1 OUTAGE OR MISLEADING DATA IN THE MICROGRID SYSTEM

Operating scenario	**Training Response**	
Type of deceived data (applied on PMU1)	***The output of Training Module I (Data Type)***	***Protection Action***
Sawtooth	PMU misleading data	The CPU will generate a deceptive data warning and remove PMU1 from the protection scheme.
Square	PMU misleading data	The CPU will generate a deceptive data warning and remove PMU1 from the protection scheme.
Ramp	PMU misleading data	The CPU will generate a deceptive data warning and remove PMU1 from the protection scheme.
3rd Harmonics Variation	PMU misleading data	The CPU will generate a deceptive data warning and remove PMU1 from the protection scheme.
5th Harmonics Variation	PMU misleading data	The CPU will generate a deceptive data warning and remove PMU1 from the protection scheme.
7th Harmonics Variation	PMU misleading data	The CPU will generate a deceptive data warning and remove PMU1 from the protection scheme.
Random	Noise in the Data	The CPU will generate a deceptive data warning and remove PMU1 from the protection scheme.
No signal	Outage	PMUs 2 and 3 are used to take further protective measures.
Missing Data	Outage	PMUs 2 and 3 are used to take further protective measures.
No Addon	Healthy	The central protection scheme will stay unchanged

TABLE II: RESPONSE OF PROPOSED TRAINING MODULE II SCHEME AGAINST VARIOUS FAULTS AND LOAD VARIATION FOR MICROGRID SYSTEM

Operating scenario		**Training Response**		***Relaying action***	***Operating Time (S)***
Fault Type	***Faulty Section***	***Output of Training Module II (a)***	***Output of Training Module II (b)***		
AB fault	S1	AB fault	S1	Disconnection of phases A and B in section S1	0.0113
BC fault	S1	BC fault	S1	Disconnection of phases B and C in section S1	0.0117
AG fault	S1	AG fault	S1	Disconnection of phases A and G in section S1	0.0115
BG fault	S1	BG fault	S1	Disconnection of phases B and G in section S1	0.0128
AB fault	S2	AB fault	S2	Disconnection of phases A and B in section S2	0.0134
BC fault	S2	BC fault	S2	Disconnection of phases B and C in section S2	0.0129
AG fault	S2	AG fault	S2	Disconnection of phases A and G in section S2	0.0132
ABG fault	S2	ABG fault	S2	Disconnection of phases A, B and G in section S2	0.0143
Load Variation	(+/_) 20 to 40%	NF	.....	No Action	.....

B. Fault Detection and Section Identification

Figure 9 illustrates the confusion matrix for fault detection and classification in Zone II (PMU 1 Outage Zone), highlighting the training performance of the ensemble bagging tree classifier with overall efficiency of 99.5%. This comparison between actual and expected faults during testing is based on the provided dataset. The class labels '1' denote the AB Fault, '2' corresponds to the ABCG Fault, '3' represents the ABC Fault, '4' indicates the AG Fault, and '5' signifies load variation or a healthy condition.

Likewise, Figure 10 depicts the confusion matrix for section identification in the PMU1 Outage Zone. If a fault occurs in Zone II while PMU1 is disabled, PMU3 on Bus 7 can be utilized to diagnose the faulty section S1. Zone II consists of two sections, with class labels '1' denoting a fault in section 1 and class labels '2' representing a fault in section 2.

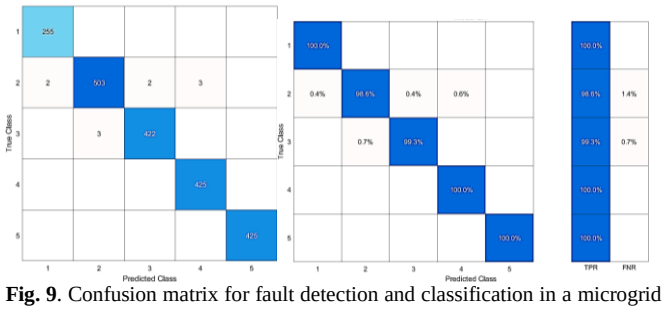

Fig. 9. Confusion matrix for fault detection and classification in a microgrid system.

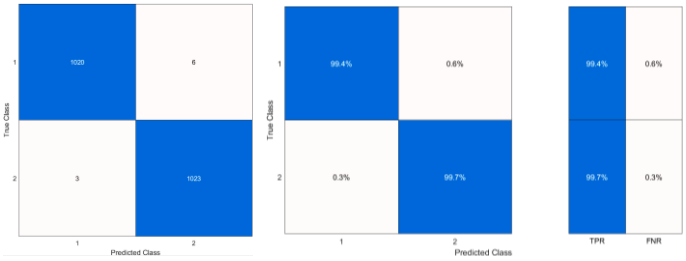

Fig. 10. Confusion matrix for identifying fault sections in the PMU outage zone (zone II) of a microgrid system.

C. Fault Detection and Section Identification: Response of Training Module II to Various Fault and Loading Conditions, and the Associated Action

Table III showcases the effectiveness of the proposed training module II, illustrated in Figure 6, across various aspects, including fault types, load fluctuations, section identification, response time, and relaying actions In microgrids with dynamic loading, the occurrence of sudden load fluctuations often leads to misinterpretations. Especially during an outage, accurately detecting faults from a considerable distance away, beyond the range of another PMU zone, poses a significant challenge. Figure 10 presents a notable scenario where a nonlinear load switching event takes place at t=0.12 sec, followed by an AB fault at t=0.2 sec in the S1 section. Despite variations in the current profile, the tripping signal for nonlinear loading is not generated. However, the AB fault with nonlinear loading is promptly identified at 0.2113 sec, demonstrating the robustness of the fault detection system.

The performance evaluation of the proposed HHT-Ensemble Bagging Tree-based protection scheme, in comparison to other classifiers, was conducted to gauge its effectiveness. The results of this comparative assessment can be found in Table III, which includes the evaluation of Support Vector Machine (SVM) and Decision Tree (DT) classifiers as well.

TABLE III: COMPARATIVE STUDY BETWEEN ENSEMBLE BAGGING TREE CLASSIFIER, SUPPORT VECTOR MACHINE AND DECISION TREE

Type of classifier		*Bagging Tree*	*Support Vector Machine (SVM)*	*Decision Tree (DT)*
Number of test cases	*Total*	4307	4307	4307
	PMU Estate Estimation	816	816	816
	Fault Detection	2465	2465	2465
	Section Identification	1026	1026	1026
Classification Accuracy	*PMU Estate Estimation*	100.00%	98.12%	99.54%
	Fault Detection	99.55%	96.48%	97.66%
	Section Identification	99.51%	97.23%	98.34%

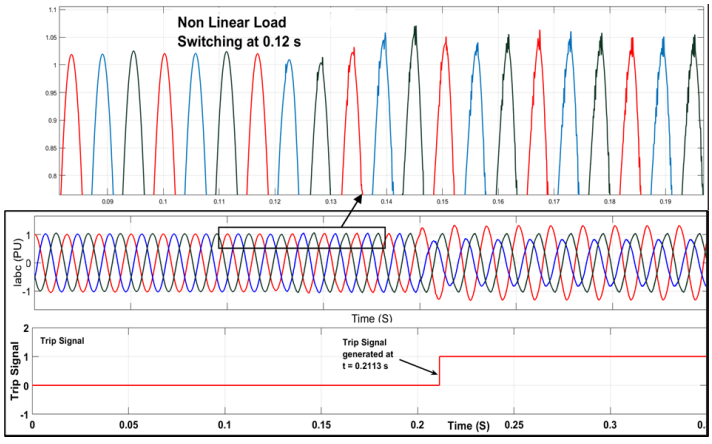

Fig. 10. Nonlinear load switching at t=0.12 s, followed by an AB fault at t = 0.2 s in the S1 section

For a comprehensive comparison, a total of 4307 test cases were meticulously analyzed, encompassing 816 PMU Estate Estimation cases, 2465 Fault Detection cases, and 1026 Section Identification cases. Remarkably, the proposed Ensemble Bagging Tree-based classifier achieved an outstanding classification accuracy of 99.5%, surpassing the results of both the SVM and DT classifiers. This clearly proves the proposed protection approach is highly effective and proficient in fulfilling its intended task.

4. CONCLUSION

This research paper introduces a highly effective adaptive machine learning approach that significantly enhances high-impedance fault (HIF) detection during PMU outages in microgrids, thereby strengthening the overall resilience of the microgrid. The combined framework of HHT and ANOVA offers an efficient feature selection method for precise PMU outage detection, HIF detection, and fault classification, showcasing the potential of machine learning in improving

microgrid protection. Simulation studies in MATLAB Simulink demonstrate the approach's effectiveness in enhancing HIF detection during PMU outages. The proposed protection scheme accurately identifies HIFs and faulty PMUs even under various misleading data or noise conditions. Furthermore, the proposed approach outperforms DT and SVM-based methods, achieving a remarkable 99.5% overall accuracy during training with the Ensemble Bagging Tree-based classifier.

REFERENCES

[1] R. B. Sharma and G. M. Dhole, "Wide Area Measurement Technology in Power Systems," *Procedia Technology*, vol. 25, 2016, doi: 10.1016/j.protcy.2016.08.165.

[2] M. Elimam, Y. J. Isbeih, M. S. El Moursi, K. Elbassioni, and K. H. Al Hosani, "Novel Optimal PMU Placement Approach Based on the Network Parameters for Enhanced System Observability and Wide Area Damping Control Capability," *IEEE Transactions on Power Systems*, vol. 36, no. 6, 2021, doi: 10.1109/TPWRS.2021.3076576.

[3] A. Bashian, M. Assili, A. Anvari-Moghaddam, and O. R. Marouzi, "Co-optimal PMU and communication system placement using hybrid wireless sensors," *Sustainable Energy, Grids and Networks*, vol. 19, 2019, doi: 10.1016/j.segan.2019.100238.

[4] M. Manohar, E. Koley, and S. Ghosh, "Microgrid protection against high impedance faults with robustness to harmonic intrusion and weather intermittency," *IET Renewable Power Generation*, vol. 15, no. 11, 2021, doi: 10.1049/rpg2.12167.

[5] F. Aminifar, C. Lucas, A. Khodaei, and M. Fotuhi-Firuzabad, "Optimal placement of phasor measurement units using immunity genetic algorithm," *IEEE Transactions on Power Delivery*, vol. 24, no. 3, 2009, doi: 10.1109/TPWRD.2009.2014030.

[6] H. H. Müller and C. A. Castro, "Genetic algorithm-based phasor measurement unit placement method considering observability and security criteria," *IET Generation, Transmission and Distribution*, vol. 10, no. 1, 2016, doi: 10.1049/iet-gtd.2015.1005.

[7] A. Asgari and K. G. Firouzjah, "Optimal PMU placement for power system observability considering network expansion and N - 1 contingencies," *IET Generation, Transmission and Distribution*, vol. 12, no. 18, 2018, doi: 10.1049/iet-gtd.2018.5874.

[8] M. K. Arpanahi, H. H. Alhelou, and P. Siano, "A Novel Multiobjective OPP for Power System Small Signal Stability Assessment Considering WAMS Uncertainties," *IEEE Trans Industr Inform*, vol. 16, no. 5, 2020, doi: 10.1109/TII.2019.2911397.

[9] Z. Miljanić, I. Djurović, and I. Vujošević, "Optimal placement of PMUs with limited number of channels," *Electric Power Systems Research*, vol. 90, 2012, doi: 10.1016/j.epsr.2012.04.010.

[10] L. Ibarra, J. Avilés, D. Guillen, J. C. Mayo-Maldonado, J. E. Valdez-Resendiz, and P. Ponce, "Optimal micro-PMU placement and virtualization for distribution network changing topologies," *Sustainable Energy, Grids and Networks*, vol. 27, 2021, doi: 10.1016/j.segan.2021.100510.

[11] N. H. A. Rahman and A. F. Zobaa, "Integrated Mutation Strategy with Modified Binary PSO Algorithm for Optimal PMUs Placement," *IEEE Trans Industr Inform*, vol. 13, no. 6, 2017, doi: 10.1109/TII.2017.2708724.

[12] T. K. Maji and P. Acharjee, "Multiple Solutions of Optimal PMU Placement Using Exponential Binary PSO Algorithm for Smart Grid Applications," *IEEE Trans Ind Appl*, vol. 53, no. 3, 2017, doi: 10.1109/TIA.2017.2666091.

[13] A. A. Saleh, A. S. Adail, and A. A. Wadoud, "Optimal phasor measurement units placement for full observability of power system using improved particle swarm optimisation," *IET Generation, Transmission and Distribution*, vol. 11, no. 7, 2017, doi: 10.1049/iet-gtd.2016.1636.

[14] M. B. Mohammadi, R. A. Hooshmand, and F. H. Fesharaki, "A new approach for optimal placement of PMUs and their required communication infrastructure in order to minimize the cost of the WAMS," *IEEE Trans Smart Grid*, vol. 7, no. 1, 2016, doi: 10.1109/TSG.2015.2404855.

[15] M. H. F. Wen, J. Xu, and V. O. K. Li, "Optimal multistage PMU placement for wide-area monitoring," *IEEE Transactions on Power Systems*, vol. 28, no. 4, 2013, doi: 10.1109/TPWRS.2013.2277741.

[16] N. C. Koutsoukis, N. M. Manousakis, P. S. Georgilakis, and G. N. Korres, "Numerical observability method for optimal phasor measurement units placement using recursive tabu search method," *IET Generation, Transmission and Distribution*, vol. 7, no. 4, 2013, doi: 10.1049/iet-gtd.2012.0377.

[17] V. Yuvaraju and S. Thangavel, "Optimal phasor measurement unit placement for power system observability using teaching–learning based optimization," *International Journal of Electrical Power and Energy Systems*, vol. 137, 2022, doi: 10.1016/j.ijepes.2021.107775.

[18] S. Heidari, S. Asgharigovar, P. Pourghasem, H. Seyedi, and Ö. Usta, "Performance evaluation of HHT and WT for detection of HIF and CT saturation in smart grids," *Turkish Journal of Electrical*

Engineering and Computer Sciences, vol. 25, no. 9, 2021, doi: 10.3906/elk-2101-8.

[19] W. C. Santos, F. V. Lopes, N. S. D. Brito, and B. A. Souza, "High-Impedance Fault Identification on Distribution Networks," *IEEE Transactions on Power Delivery*, vol. 32, no. 1, 2017, doi: 10.1109/TPWRD.2016.2548942.

[20] M. Manohar, E. Koley, and S. Ghosh, "Microgrid protection against high impedance faults with robustness to harmonic intrusion and weather intermittency," *IET Renewable Power Generation*, vol. 15, no. 11, 2021, doi: 10.1049/rpg2.12167.

[21] K. Sekar and N. K. Mohanty, "Data mining-based high impedance fault detection using mathematical morphology," *Computers and Electrical Engineering*, vol. 69, 2018, doi: 10.1016/j.compeleceng.2018.05.010.

[22] Q. Cui and Y. Weng, "Enhance High Impedance Fault Detection and Location Accuracy via \mu -PMUs," *IEEE Trans Smart Grid*, vol. 11, no. 1, 2020, doi: 10.1109/TSG.2019.2926668.

[23] S. F. Zargar, M. M. Farsangi, and M. Zare, "Probabilistic multi-objective state estimationbased PMU placement in the presence of bad data and missing measurements," *IET Generation, Transmission and Distribution*, vol. 14, no. 15, 2020, doi: 10.1049/iet-gtd.2019.1317.

[24] J. Dagle, "The North American SynchroPhasor Initiative (NASPI)," in *IEEE PES General Meeting, PES 2010*, 2010. doi: 10.1109/PES.2010.5590048.

[25] H. Lin *et al.*, "Self-healing attack-resilient PMU network for power system operation," *IEEE Trans Smart Grid*, vol. 9, no. 3, 2018, doi: 10.1109/TSG.2016.2593021.

[26] M. Shaik, A. G. Shaik, and S. K. Yadav, "Hilbert–Huang transform and decision tree based islanding and fault recognition in renewable energy penetrated distribution system," *Sustainable Energy, Grids and Networks*, vol. 30, 2022, doi: 10.1016/j.segan.2022.100606.

Mr. Laxman Solankee

Mr, Laxman Solankeev earned his B.E. degree from Rajiv Gandhi Proudyogiki Vishwavidyalaya, Bhopal M.P., India, in 2007, followed by his M.Tech degrees from MANIT, Bhopal, India, in 2009. Since 2019, he has been a research scholar in the Department of Electrical Engg. at University Institute of Technology, RGPV, Bhopal M.P. he has a commendable record of publications in high-impact factor journals and various renowned international conferences. His research interests encompass Microgrid protection, Renewable Energy Resources, and the application of soft computing and data mining in power system protection.

Dr. Avinash Rai

Dr. Avinash Rai B.E (Electronics), M.E (VLSI Design), Ph. D (Wireless Sensor Networks) currently works as an Assistant Professor in Department of Electronics & Communication Engg. University Institute of Technology, Rajiv Gandhi Proudyogiki Vishwavidyalaya, Bhopal M.P. Dr. Avinash does research in Wireless Sensor Networks, Telecommunications Engineering and Electronic Engineering. Their most recent publication is 'Enhancing Energy of Sensor Node to increase efficiency in Wireless Sensor Network'.

Dr. Mukesh Kumar Kirar

Mukesh Kumar Kirar (Senior Member, IEEE) received the B.E. degree from the Government Engineering College, Ujjain, India, in 2006, and the M.Tech. and Ph.D. degrees from the MANIT, Bhopal, India, in 2008 and 2014, respectively. Since 2010, he has been working as an Assistant Professor with the Department of Electrical Engineering, MANIT. He has more than 13 years of industry and teaching experience. He has several publications in high-impact factor journals and various international conferences of repute. His research interests include industrial power system design and analysis, load shedding design, optimization techniques, artificial neural networks, and power system protection. He is a reviewer of various esteemed journals.